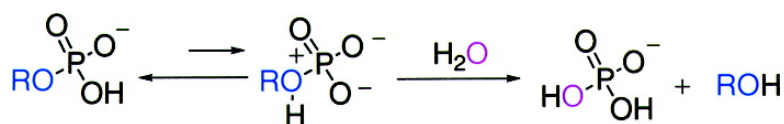


## Transition State Differences in Hydrolysis Reactions of Alkyl versus Aryl Phosphate Monoester Monoanions

Piotr K. Grzyska, Przemyslaw G. Czyryca, Jamie Purcell, and Alvan C. Hengge

*J. Am. Chem. Soc.*, **2003**, 125 (43), 13106-13111 • DOI: 10.1021/ja036571j • Publication Date (Web): 01 October 2003

Downloaded from <http://pubs.acs.org> on March 30, 2009



### More About This Article

Additional resources and features associated with this article are available within the HTML version:

- Supporting Information
- Links to the 4 articles that cite this article, as of the time of this article download
- Access to high resolution figures
- Links to articles and content related to this article
- Copyright permission to reproduce figures and/or text from this article

[View the Full Text HTML](#)



## Transition State Differences in Hydrolysis Reactions of Alkyl versus Aryl Phosphate Monoester Monoanions

Piotr K. Grzyska, Przemyslaw G. Czyryca, Jamie Purcell, and Alvan C. Hengge\*

Contribution from the Utah State University, Department of Chemistry and Biochemistry,  
Logan, Utah 84322-0300

Received June 9, 2003; E-mail: hengge@cc.usu.edu.

**Abstract:** Although aryl phosphates have been the subject of numerous experimental studies, far less data bearing on the mechanism and transition states for alkyl phosphate reactions have been presented. Except for esters with very good leaving groups such as 2,4-dinitrophenol, the monoanion of phosphate esters is more reactive than the dianion. Several mechanisms have been proposed for the hydrolysis of the monoanion species.  $^{18}\text{O}$  kinetic isotope effects in the nonbridging oxygen atoms and in the P–O(R) ester bond, and solvent deuterium isotope effects, have been measured for the hydrolysis of *m*-nitrobenzyl phosphate. The results rule out a proposed mechanism in which the phosphoryl group deprotonates water and then undergoes attack by hydroxide. The results are most consistent with a preequilibrium proton transfer from the phosphoryl group to the ester oxygen atom, followed by rate-limiting P–O bond fission, as originally proposed by Kirby and co-workers in 1967. The transition state for *m*-nitrobenzyl phosphate (leaving group  $\text{p}K_{\text{a}}$  14.9) exhibits much less P–O bond fission than the reaction of the more labile *p*-nitrophenyl phosphate (leaving group  $\text{p}K_{\text{a}}$  = 7.14). This seemingly anti-Hammond behavior results from weakening of the P–O(R) ester bond resulting from protonation, an effect which calculations have shown is much more pronounced for aryl phosphates than for alkyl ones.

### Introduction

The chemistry of phosphate monoesters forms the basis for the regulation of a host of biochemical processes, accounting in part for the intense interest in these compounds. Much of what is known regarding the mechanisms of phosphoryl transfer and their transition states has been inferred from experiments using aryl phosphate esters. Conversely, most of the computational work has been performed using methyl phosphate. We report solvent isotope effects, and  $^{18}\text{O}$  isotope effects in the leaving group and in the phosphoryl group for the hydrolysis of the alkyl phosphate *m*-nitrobenzyl phosphate (*m*NBP). The results provide a basis for choosing among various mechanistic proposals. In addition, comparison with data obtained previously for *p*-nitrophenyl phosphate reveal differences in the transition state of the hydrolysis of the aryl versus the alkyl ester.

Depending upon pH, phosphate monoesters exist either as the monoanion or the dianion (except at very low pH values where the neutral species exists). With the exception of esters with highly activated leaving groups such as 2,4-dinitrophenol, the monoanion species is much more reactive than the dianion.<sup>1</sup> A large body of experimental evidence indicates that the reactions of dianions are concerted with loose, metaphosphate-like transition states.<sup>2</sup> In reactions of monoanions, linear free energy relationships<sup>1</sup> and kinetic isotope effects<sup>3</sup> with aryl

phosphates indicate that the leaving group is largely neutral in the transition state, implying that P–O bond fission is accompanied by protonation of the leaving group. Linear free energy relationships with monoanionic phosphorylated pyridines have been interpreted to indicate a loose transition state in which metaphosphate is not an intermediate.<sup>4</sup> The hydrolysis of the monoanion of 2,4-dinitrophenyl phosphate is thought to be concerted,<sup>5</sup> but the possibility of a metaphosphate intermediate has not been ruled out with esters having less activated leaving groups. A stereochemical study of the hydrolysis of phenyl phosphate monoanion indicates the reaction proceeds with inversion.<sup>6</sup> Such a result is consistent either with a concerted mechanism, or with a discrete metaphosphate intermediate in a preassociative mechanism. The results reported here do not address this question, but rather, examine the timing and synchronicity of proton transfer and P–O bond fission to the leaving group.

Kirby<sup>1</sup> postulated that protonation of the leaving group accompanies deprotonation of the phosphoryl group (probably via the intermediacy of one or more water molecules) and considered the timing of the proton transfer (Figure 1). He concluded that for less basic leaving groups, protonation occurs simultaneously with leaving group departure and is partially rate-limiting, whereas for more basic leaving groups, a bridge-protonated intermediate forms followed by rate-limiting P–O bond fission. Consistent with this proposal, a solvent isotope

(1) Kirby, A. J.; Varvoglis, A. G. *J. Am. Chem. Soc.* **1967**, *89*, 415.  
(2) Thatcher, G. R. J.; Kluger, R. *Adv. Phys. Org. Chem.* **1989**, *25*, 99; Hengge, A. C. In *Comprehensive Biological Catalysis: A Mechanistic Reference*; Sinnott, M., Ed.; Academic Press: San Diego, CA, 1998; Vol. 1, p 517.  
(3) Hengge, A. C.; Edens, W. A.; Elsing, H. *J. Am. Chem. Soc.* **1994**, *116*, 5045.

(4) Herschlag, D.; Jencks, W. P. *J. Am. Chem. Soc.* **1989**, *111*, 7579.  
(5) Admiraal, S. J.; Herschlag, D. *J. Am. Chem. Soc.* **2000**, *122*, 2145.  
(6) Buchwald, S. L.; Friedman, J. M.; Knowles, J. R. *J. Am. Chem. Soc.* **1984**, *106*, 4911.

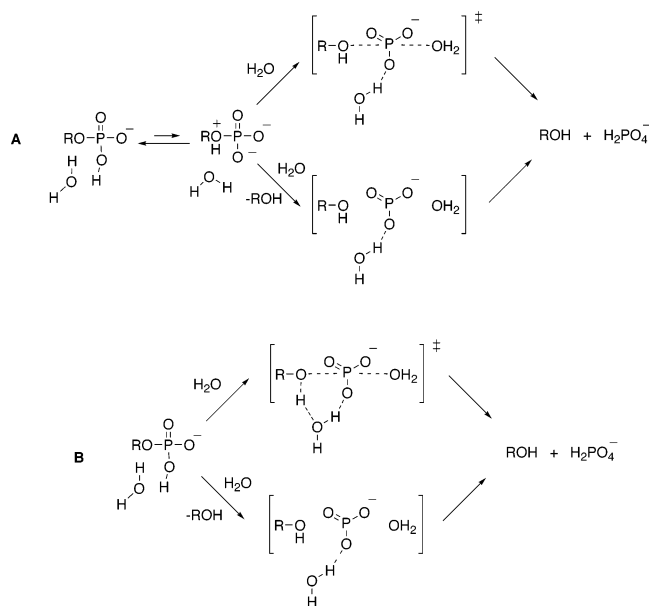


**Figure 1.** Possible mechanisms for hydrolysis of monoanions of phosphate monoesters. In mechanism A proton transfer from the phosphoryl group (probably via the intermediacy of a water molecule) yields an anionic zwitterion intermediate. This may react in either concerted fashion (upper pathway) or via a discrete metaphosphate intermediate in a preassociative mechanism (bottom pathway). Mechanism B denotes proton-transfer concerted with P–O bond fission. As with A, such a mechanism could either occur with concerted phosphoryl transfer to the nucleophile (upper pathway) or via a discrete metaphosphate intermediate in a preassociative mechanism (bottom pathway).

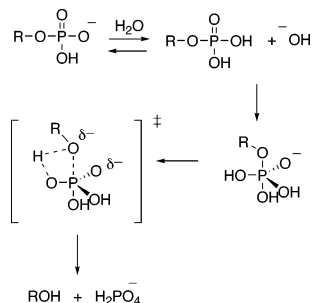


**Figure 2.** In this proposed mechanism for monoanion hydrolysis the protonated, neutral phosphate ester is attacked by hydroxide to form a pentacoordinate phosphorane intermediate.

effect of 1.45 is found for hydrolysis of the monoanion of 2,4-dinitrophenyl phosphate at 39 °C,<sup>1</sup> whereas the figure for methyl phosphate is 0.87 at 100 °C.<sup>7</sup>

Computational results favoring several alternative mechanisms for the hydrolysis of phosphate monoester monoanions have been presented.<sup>8–11</sup> One such proposal<sup>8</sup> is an associative mechanism for the hydrolysis of methyl phosphate monoanion, in which the reactant is protonated and subsequently attacked by hydroxide to form a pentacoordinate intermediate, the breakdown of which is rate-determining (Figure 2). This proposal has been controversial, with criticisms<sup>5</sup> and counterarguments<sup>12</sup> presented.

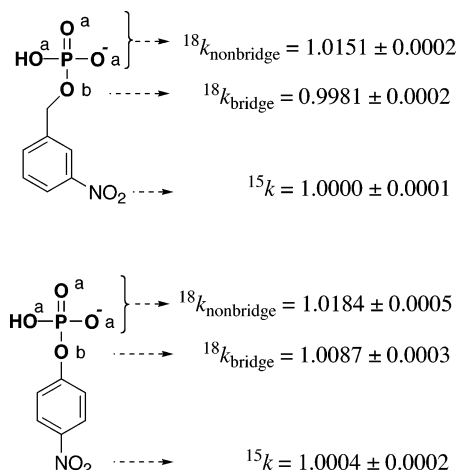


**Figure 3.** Measured <sup>18</sup>O and <sup>15</sup>N KIEs for hydrolysis of the monoanions of *m*-nitrobenzyl phosphate (top, this study) and *p*-nitrophenyl phosphate<sup>15</sup> (bottom), measured at their respective pH-optima. For *m*-NBP, pH 4.0, 115 °C. For *p*NPP, pH 3.5, 95 °C. Nonbridging oxygen atoms are designated by “a”, bridging ones by “b”. The KIE of unity measured at the nitrogen atom of *m*-nitrobenzyl phosphate is expected, since no charge delocalization or other bonding changes involving this atom occur during the reaction.

In another computational study,<sup>9</sup> the hydrolysis of methyl phosphate monoanion was examined with the inclusion of explicitly modeled solvating water molecules, and a dissociative pathway was favored. Proton transfer to the leaving group and P–O bond fission occur in the same step in the favored mechanism, with proton transfer more advanced than P–O bond fission. Calculations by others<sup>10,11</sup> favor the intermediacy of a bridge-protonated intermediate in the hydrolysis of the methyl phosphate monoanion, as originally proposed by Kirby and Varvoglis. The bridge-protonated anionic zwitterions of methyl and of phenyl phosphate were found to exist as viable intermediates, whereas the corresponding anionic zwitterion of 2,4-dinitrophenyl phosphate was not,<sup>10</sup> implying that the transition from mechanisms A to B in Figure 1 occurs somewhere in between. In a computational examination of the effect of the protonation state on the hydrolysis mechanisms of phosphate esters,<sup>13</sup> it was concluded that a dissociative mechanism is favored when the phosphoryl group is fully deprotonated, whereas an associative one is favored for neutral esters.

We have measured the solvent deuterium and <sup>18</sup>O kinetic isotope effects (KIEs) on the hydrolysis of *m*-nitrobenzyl phosphate (leaving group p*K*<sub>a</sub> = 14.9<sup>14</sup>) for comparison with previously reported data on the hydrolysis of *p*-nitrophenyl phosphate (pNPP)<sup>15</sup> (leaving group p*K*<sub>a</sub> = 7.14). The <sup>18</sup>O KIEs were measured by the remote label method, using the nitrogen atom as a reporter for isotopic fractionation at the nonbridging, or bridging, oxygen positions.<sup>15</sup> Figure 3 shows the reactant and the positions at which KIEs were measured.

The protonation or deprotonation of the phosphoryl group will directly influence the <sup>18</sup>k<sub>nonbridge</sub> KIE. Deprotonation of phosphate monoesters is accompanied by a normal <sup>18</sup>k<sub>nonbridge</sub> equilibrium isotope effect (EIE) of 1.015.<sup>16</sup> In hydrolysis reactions, <sup>18</sup>k<sub>nonbridge</sub> will also have a secondary contribution from

(7) Buntton, C. A.; Llewellyn, D. R.; Oldham, K. G.; Vernon, C. A. *J. Chem. Soc.* **1958**, 3574.

(8) Florian, J.; Warshel, A. *J. Am. Chem. Soc.* **1997**, *119*, 5473; Florian, J.; Warshel, A. *J. Phys. Chem. B* **1998**, *102*, 719.

(9) Hu, C.-H.; Brinck, T. *J. Phys. Chem. A* **1999**, *103*, 5379.

(10) Bianciotto, M.; Barthelat, J.-C.; Vigroux, A. *J. Phys. Chem. A* **2002**, *106*, 6521.

(11) Bianciotto, M.; Barthelat, J.-C.; Vigroux, A. *J. Am. Chem. Soc.* **2002**, *124*, 7573.

(12) Glennon, T. M.; Villa, J.; Warshel, A. *Biochemistry* **2000**, *39*, 9641.

(13) Wilkie, J.; Gani, D. *J. Chem. Soc., Perkin Trans. 2* **1996**, 783.

(14) Sowa, G. A.; Hengge, A. C.; Cleland, W. W. *J. Am. Chem. Soc.* **1997**, *119*, 2319.

(15) Hengge, A. C. *Acc. Chem. Res.* **2002**, *35*, 105.

(16) Knight, W. B.; Weiss, P. M.; Cleland, W. W. *J. Am. Chem. Soc.* **1986**, *108*, 2759.

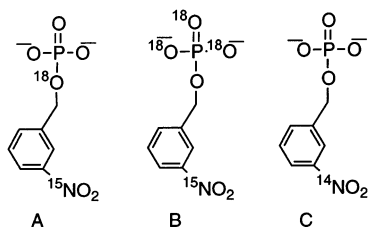


**Figure 4.** Isotopic isomers synthesized for measurement of the bridge (A and C) and nonbridge (B and C)  $^{18}\text{O}$  isotope effects.

the hybridization change at phosphorus depending on whether the transition state for phosphoryl transfer is loose or tight. Loose transition states typical of monoester dianion reactions result in small inverse secondary  $^{18}k_{\text{nonbridge}}$  KIEs,<sup>15</sup> whereas the tight, phosphorane-like transition states of triester reactions result in normal  $^{18}k_{\text{nonbridge}}$  KIEs, up to 1.03.<sup>17</sup>

The  $^{18}k_{\text{bridge}}$  KIE is sensitive to the degree of fission of the P–O bond in the transition state. The solvent isotope effects give an indication of whether a proton is in flight in the transition state of the rate-limiting step.

### Experimental Section

The materials, reagents, and solvents were commercial products and were used as received unless otherwise noted. *m*-Nitrobenzyl alcohol was distilled under reduced pressure. Acetonitrile was distilled from phosphorus pentoxide. Carbon tetrachloride and phosphorus trichloride were redistilled. Mercury (II) chloride was sublimed under reduced pressure. Phosphorous acid was dried under reduced pressure. Triethylamine was stored over potassium hydroxide. All solid reactants were kept in desiccators over phosphorus pentoxide.

The commercially available bis(cyclohexylammonium) salt of *p*-nitrophenyl phosphate was recrystallized before use. The disodium salt of methyl phosphate was synthesized by a literature method.<sup>18</sup> The synthesis of bis(cyclohexylammonium) salt of *m*-nitrobenzyl phosphate is described below.

The isotopic isomers of *m*-nitrobenzyl phosphate used for measurement of kinetic isotope effects are shown in Figure 4. A mixture of isotopic isomers A and C was used for determination of  $^{18}k_{\text{bridge}}$ . Isomers B and C were mixed to reconstitute the natural abundance of  $^{15}\text{N}$  and used for determination of  $^{18}k_{\text{nonbridge}}$ . The isotopic abundance of the mixtures was determined by isotope ratio mass spectrometry.

[ $^{14}\text{N}$ ] labeled *m*-nitrobenzyl alcohol, [ $^{15}\text{N}$ ] labeled *m*-nitrobenzyl alcohol, and [ $^{15}\text{N}$ ,  $^{18}\text{O}$ ] labeled *m*-nitrobenzyl alcohol were synthesized as described previously.<sup>14</sup>

**$^{18}\text{O}$ -Labeled Phosphorous Acid ( $\text{H}_3\text{P}^{18}\text{O}_3$ ).** A modification of a published procedure<sup>19</sup> was used. A 50 mL Claisen flask was fitted with a condenser under dry nitrogen and placed in an ice bath. Carbon tetrachloride (1.6 mL) and phosphorus trichloride (0.33 mL, 1 eq.) were added and vigorously mixed. Into this mixture, [ $^{18}\text{O}$ ]-water (0.22 mL, 2.8 eq.) was added over about 1 h in such a manner that overheating was avoided. The ice bath was then removed and the reaction mixture stirred for one more hour. Volatile materials were subsequently removed under vacuum, leaving crystalline phosphorous acid (0.31 g, 95% yield).

**Natural Abundance *m*-Nitrobenzyl Phosphate.** This was synthesized by a modification of a published procedure.<sup>20</sup> In a 500 mL three neck flask fitted with reflux condenser and large stirrer, *m*-nitrobenzyl alcohol (25 g, 6 equiv), 1,8-diazobicyclo-[5.4.0]-undec-7-ene (19.9 g, 4.1equiv), and phosphorous acid (2.68 g, 1 equiv) were mixed with

150 mL of acetonitrile. To this mixture was introduced mercury (II) chloride (10 g, 1.1 equiv) dissolved in acetonitrile (150 mL) via an addition funnel. After addition was complete, the reaction was rapidly brought to boiling and stirred vigorously for about 30 min. Water (100 mL) was injected to the reaction mixture, and the flask was cooled to room temperature. The reaction mixture was filtered and the acetonitrile removed by rotary evaporation. The remaining aqueous mixture was titrated to pH 13 using sodium hydroxide and extracted with chloroform.  $^{31}\text{P}$  NMR showed the presence of *m*-nitrobenzyl phosphate and inorganic phosphate in a ratio of about 9:1. The *m*-nitrobenzyl phosphate was purified by anion exchange using DEAE Sephadex eluting with an ammonium bicarbonate/water gradient, starting with water and ending with 0.7 M ammonium bicarbonate. Fractions containing *m*-nitrobenzyl phosphate were pooled and ammonium bicarbonate removed by repeated rotary evaporation with isopropyl alcohol. The product was titrated to pH 9 with cyclohexylamine, dried and recrystallized from isopropyl alcohol/5% cyclohexylamine. The product, dicyclohexylammonium *m*-nitrobenzyl phosphate was 10.9 g, which is 78% yield from phosphorous acid. A sample was converted to the sodium salt and analyzed by NMR:  $^1\text{H}$  NMR (400 MHz,  $\text{D}_2\text{O}$ )  $\delta$  8.40 (s, 1H), 8.27 (d, 1H,  $J = 8.2$ ), 7.95 (d, 1H,  $J = 7.7$ ), 7.72 (t, 1H,  $J = 8.0$ ), 5.00 (d, 2H,  $J = 5.9$  Hz),  $^{31}\text{P}$  NMR (162 MHz, 85% phosphoric acid reference)  $\delta$  1.5

[ $^{14}\text{N}$ ]-*m*-Nitrobenzyl Phosphate was prepared in a similar manner, using [ $^{14}\text{N}$ ]-*m*-nitrobenzyl alcohol.

**Mixture of Isotopic Isomers A and C.** [ $^{14}\text{N}$ ]-*m*-nitrobenzyl alcohol and [ $^{15}\text{N}$ ,  $^{18}\text{O}$ ]-*m*-nitrobenzyl alcohol were mixed to reconstitute the natural abundance of  $^{15}\text{N}$ , and then the mixture was phosphorylated using the method cited above to produce a mixture of isotopic isomers A and C (Figure 4).

**[ $^{15}\text{N}$ , Nonbridge- $^{18}\text{O}_3$ ] *m*-Nitrobenzyl Phosphate.** This was prepared in the same manner as the natural abundance compound, on a 1/100 scale, using [ $^{18}\text{O}$ ] labeled phosphorous acid and [ $^{15}\text{N}$ ]-*m*-nitrobenzyl alcohol. The level of  $^{18}\text{O}$  incorporation was determined by FAB-MS (see the Supporting Information for levels of isotopic incorporation of all labeled compounds).

**Isotope Effect Determinations.** Isotope effects were measured by isotope ratio mass spectrometry. The  $^{15}\text{N}$  isotope effects were measured using the natural abundance compound. The  $^{18}\text{O}$  isotope effects were measured by the remote label method using the nitrogen atom as a reporter for isotopic fractionation at the bridge or nonbridge oxygen atoms. The experimental procedures used to measure these isotope effects were similar to those previously reported to measure KIEs in phosphoryl transfer reactions in which the leaving group is *p*-nitrophenol.<sup>15</sup> In summary, the reactions were carried out using  $\sim 100$   $\mu\text{moles}$  of *m*NBP at pH 4.0 in acetate buffer at 115  $^\circ\text{C}$ , stopped after partial completion by chilling, and assayed by  $^{31}\text{P}$  NMR to determine the precise fraction of reaction. The *m*-nitrobenzyl alcohol product from this first portion of the reaction was separated from the unreacted ester. The unreacted ester was completely hydrolyzed, and the *m*-nitrobenzyl alcohol released in the second portion of the reaction was isolated. Both samples of *m*-nitrobenzyl alcohol were purified and subjected-to-isotope ratio analysis. The details of the experimental procedures and the data analysis are given in Supporting Information.

**Solvent Deuterium Isotope Effects.** Buffered solutions of the reactants were prepared in parallel containing 20 mL of 25mM phosphate ester in 250mM succinic acid buffer at pH 4.0. This solution was divided into two separate flasks and dried in vacuo at ambient temperature. The dry mixtures of buffer and phosphate ester were reconstituted in either  $\text{H}_2\text{O}$  or  $\text{D}_2\text{O}$ . The pH for the  $\text{D}_2\text{O}$ -reconstituted buffer was found to obey the expected formula  $\text{pD} = \text{meter reading} + 0.4$ . Samples of the reaction mixtures were removed at time intervals and assayed. The hydrolyses of methyl phosphate and of *m*-nitrobenzyl phosphate were monitored by  $^{31}\text{P}$  NMR spectroscopy. The hydrolysis of *p*-nitrophenyl phosphate was followed by UV-vis spectrophotometry

(17) Anderson, M. A.; Shim, H.; Raushel, F. M.; Cleland, W. W. *J. Am. Chem. Soc.* **2001**, *123*, 9246.

(18) Grzyska, P. K.; Czyryca, P. G.; Golightly, J.; Small, K.; Larsen, P.; Hoff, R. H.; Hengge, A. C. *J. Org. Chem.* **2002**, *67*, 1214.

(19) Voigt, D.; Gallais, F. In *Inorganic Syntheses*; New York, 1953; Vol. 4, p 55.

(20) Obata, T.; Mukaiyama, T. *J. Org. Chem.* **1967**, *32*, 1063.

at 400 nm by periodically adding an aliquot of the reaction mixture to cuvette containing 0.1N NaOH. Reactions were followed to completion, and obeyed pseudo first-order kinetics. Rate constants were determined from fits of these data to the first-order rate equation.

**Choice of Buffers.** Acetate and succinate were used as buffers in experiments at elevated temperatures because both exhibit a negligible temperature dependence on  $pK_a$  (acetate:  $\Delta pK_a/\text{°C} = 0.0002$ ; succinate:  $\Delta pK_a/\text{°C} = 0.0$ ).<sup>21</sup>

**Computational Methods.** The Gaussian 98 program<sup>22</sup> was used for the geometry optimizations and the calculations of the appropriate Hessians. The B3LYP/6-31+G\* method was employed, and all calculations applied to the molecules in the gas phase. Geometry optimization calculations were performed on the structures of *p*-nitrophenyl phosphate, *p*-nitrophenyl acetate, and *p*-nitrophenol. The optimizations were followed by calculations of Hessians, then the calculated force constants were used to calculate vibrational frequencies of the isotopically substituted species. Equilibrium isotope effects were calculated according to the Bigeleisen equation.<sup>23</sup> The Isoeff program, developed by Prof. P. Paneth, was used in these calculations.

**<sup>18</sup>O Tracer Experiments.** Solutions were prepared containing 50 mM *m*-nitrobenzyl phosphate, or inorganic phosphate, and 250 mM succinate or acetate buffer at pH 4.0 containing 30% of <sup>18</sup>O-labeled water. These solutions also contained 5% D<sub>2</sub>O to provide a lock to facilitate acquisition of NMR spectra. Reaction mixtures were sealed in high-pressure NMR tubes, and placed in an oil bath at 115 °C for 14 h. After cooling, the reaction samples were neutralized with 4N KOH, and 1 mg of EDTA was added before <sup>31</sup>P NMR analysis of the products. Integrations of overlapping peaks were obtained by Gaussian curve fitting. The *m*-nitrobenzyl alcohol product was extracted with ether and analyzed by GC–MS.

**$pK_a$  Determination.** Solutions of *m*-nitrobenzyl phosphate were prepared at pH values ranging from 4.0 to 9.0, containing 25mM *m*NBP in 100 mM acetate, 100 mM Bis-Tris or 100 mM Tris buffers. The pH values were measured using a glass electrode at 25 °C. The  $pK_a$  value was calculated from a fit of the plot of <sup>31</sup>P NMR chemical shift vs pH.

**Thermodynamic Data.** Reaction solutions containing 30 mL of 25mM *m*-nitrobenzyl phosphate ester in 250mM succinic acid buffer at pH 4.0 in thick-walled glass vessels with a pressure cap were placed in an oil bath maintained at appropriate temperature. The experiments were carried out at 95, 110, 115, 120, 125, and 130 °C. The pH was checked again at the end of the reaction and was found to be the same within  $\pm 0.05$  pH units. <sup>31</sup>P NMR was used to follow the reaction rates for four or more half-lives. Rate constants were obtained from fits of these data to the first-order rate equation. These rate constants were used to construct the Eyring plot (see the Supporting Information) which yielded a value for the enthalpy of activation of  $40 \pm 1$  kcal/mol and an entropy of activation of  $+28 \pm 1$  eu.

## Results and Discussion

**General Mechanistic Considerations.** The hydrolysis of benzyl phosphate has been studied by Westheimer and by Van Etten.<sup>24,25</sup> In that study, isotope tracer results at 75 °C showed

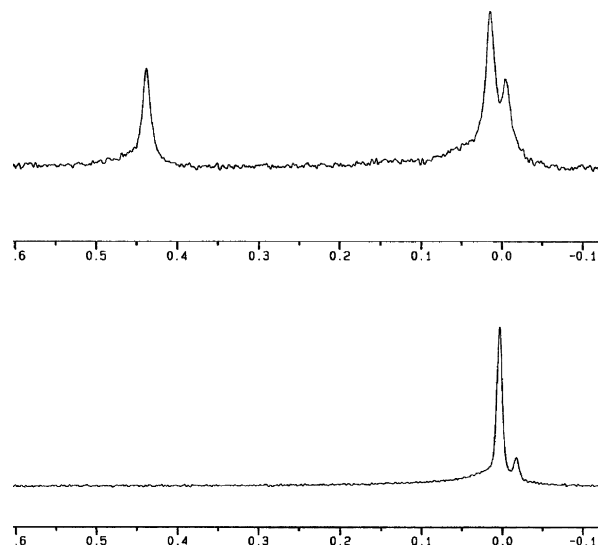


**Figure 5.** <sup>31</sup>P NMR after partial hydrolysis of *m*NBP monoanion at 115 °C (top) showing remaining *m*NBP (left) and inorganic phosphate product (right). The isotope shift is that expected from incorporation of a single atom of <sup>18</sup>O. The bottom spectrum shows inorganic phosphate after incubation under the same conditions. Extended incubation times at higher temperature results in additional incorporation of <sup>18</sup>O into inorganic phosphate (data not shown).

that nucleophilic attack occurs at phosphorus with P–O bond fission at pH 4, whereas at pH values  $< 2$ , attack at carbon (with C–O bond fission) increasingly predominates.<sup>25</sup> At pH 4, the concentration of the monoanionic species is at its highest; at lower pH, the concentration of the fully neutral species increases, resulting in the mechanistic change.

A second  $pK_a$  of 6.2 was found for *m*NBP, a value that is typical for alkyl phosphate monoesters. The hydrolysis of *m*NBP at pH 4.0 at 115 °C in water containing 30% H<sub>2</sub><sup>18</sup>O shows that at about 67% of reaction, the <sup>31</sup>P NMR signal for the inorganic phosphate product exhibits a second peak  $\sim 0.02$  ppm upfield, a shift of the magnitude expected from the incorporation of a single atom of <sup>18</sup>O<sup>26</sup> (Figure 5, top). Deconvolution and integration of these peaks showed that the inorganic phosphate product contained 42% <sup>18</sup>O. There was no detectable incorporation of <sup>18</sup>O into unreacted *m*NBP (Figure 5, top). A control experiment, in which inorganic phosphate was incubated under the same conditions for the same time duration, showed that 13% of the phosphate had incorporated <sup>18</sup>O from exchange with solvent (Figure 5, bottom). These results show that under these conditions exchange with inorganic phosphate occurs more slowly than hydrolysis of *m*NBP, but at a rate that is sufficient to account for the excess <sup>18</sup>O observed in the phosphate product. No incorporation of <sup>18</sup>O into the *m*-nitrobenzyl alcohol product could be detected by mass spectrometry. Thus, the reaction of *m*NBP at pH 4.0 proceeds by the same mechanism as that previously documented for benzyl phosphate,<sup>25</sup> namely, attack at phosphorus with P–O bond fission.

**Isotope Effects. Solvent Isotope Effects.** The solvent deuterium KIEs ( $k_{H_2O}/k_{D_2O}$ ) measured in this study are shown in Table 1. The value of 0.81 for methyl phosphate at 120 °C is close to the previously reported value of 0.87 at 101 °C.<sup>7</sup> All of the  $k_{H_2O}/k_{D_2O}$  values are slightly inverse, more suggestive of

(21) Stoll, V. S.; Blanchard, J. S. In *Guide to Protein Purification*; Deutscher, M. P., Ed.; Academic Press: San Diego, CA, 1990; Vol. 182, p 27.

(22) Frisch, M. J.; Trucks, G. W.; Schlegel, H. B.; Scuseria, G. E.; Robb, M. A.; Cheeseman, J. R.; Zakrzewski, V. G.; Montgomery, J. A., Jr.; Stratmann, R. E.; Burant, J. C.; Dapprich, S.; Millam, J. M.; Daniels, A. D.; Kudin, K. N.; Strain, M. C.; Farkas, O.; Tomasi, J.; Barone, V.; Cossi, M.; Cammi, R.; Mennucci, B.; Pomelli, C.; Adamo, C.; Clifford, S.; Ochterski, J.; Petersson, G. A.; Ayala, P. Y.; Cui, Q.; Morokuma, K.; Malick, D. K.; Rabuck, A. D.; Raghavachari, K.; Foresman, J. B.; Cioslowski, J.; Ortiz, J. V.; Stefanov, B. B.; Liu, G.; Liashenko, A.; Piskorz, P.; Komaromi, I.; Gomperts, R.; Martin, R. L.; Fox, D. J.; Keith, T.; Al-Laham, M. A.; Peng, C. Y.; Nanayakkara, A.; Gonzalez, C.; Challacombe, M.; Gill, P. M. W.; Johnson, B. G.; Chen, W.; Wong, M. W.; Andres, J. L.; Head-Gordon, M.; Replogle, E. S.; Pople, J. A. *Gaussian 98*; Gaussian, Inc.: Pittsburgh, PA, 1998.

(23) Bigeleisen, J. *J. Chem. Phys.* **1949**, *17*, 675.

(24) Kumamoto, J.; Westheimer, F. H. *J. Am. Chem. Soc.* **1955**, *77*, 2515.

(25) Parente, J. E.; Riskey, J. M.; Van Etten, R. L. *J. Am. Chem. Soc.* **1984**, *106*, 8156.

(26) Cohn, M.; Hu, A. *Proc. Natl. Acad. Sci.* **1978**, *75*, 200.

**Table 1.** Solvent Deuterium Kinetic Isotope Effects for Hydrolysis Reactions of Phosphate Monoesters Measured in This Study<sup>a</sup>

| reactant   | $k_{\text{H}_2\text{O}}/k_{\text{D}_2\text{O}}$ |
|--|---|
| <i>p</i> -nitrophenyl phosphate<br>(pH 3.5, 95°C)  | 0.96 ± 0.01                                     |
| <i>p</i> -nitrophenyl phosphate<br>(pH 4.0, 95°C)  | 0.95 ± 0.01                                     |
| <i>m</i> -nitrobenzyl phosphate<br>(pH 4.0, 110°C) | 0.94 ± 0.01                                     |
| methyl phosphate<br>(pH 4.0, 120°C)                | 0.81 ± 0.01                                     |

<sup>a</sup> The pH-optimum for the alkyl phosphates is 4.0; that for *p*-NPP is 3.5.

fractionation factors rather than the normal values expected when a proton is in flight in the transition state (for example,  $k_{\text{H}_2\text{O}}/k_{\text{D}_2\text{O}} = 1.45$  for hydrolysis of 2,4-dinitrophenyl phosphate monoanion<sup>1</sup>). The magnitudes of such KIEs can be reduced when there is a large difference in  $\text{p}K_{\text{a}}$  between the proton donor and acceptor (resulting in a very early or late transition state for proton transfer),<sup>27</sup> or by the contribution of heavy-atom motion to the reaction coordinate.<sup>28</sup> However, to our knowledge there is no precedent for such factors to completely eliminate the normal deuterium KIE expected from a proton in flight in the transition state.

**<sup>18</sup>O Isotope Effects.** The  $^{18}k_{\text{nonbridge}}$  of 1.0151 (Figure 3) for the hydrolysis of the monoanion of *m*NBP is indistinguishable from the <sup>18</sup>O equilibrium isotope effect (EIE) of 1.015 for the deprotonation of a phosphate ester.<sup>16</sup> Although the elevated temperature necessitated by the slow reaction rate of *m*NBP will slightly reduce the observed value of  $^{18}k_{\text{nonbridge}}$  this effect is relatively small and does not affect the present discussion. (An estimation of the magnitude of this reduction can be inferred from previously reported values for  $^{18}k_{\text{nonbridge}}$  for the monoanion of *p*NPP at 95 °C ( $1.0184 \pm 0.0003$ ) and at 30 °C ( $1.0199 \pm 0.0005$ )<sup>29</sup>) Protonation of the phosphoryl group such as in the mechanistic proposal of Figure 2 would result in an inverse  $^{18}k_{\text{nonbridge}}$  of similar magnitude (0.985). Even if the added proton were partially removed in a subsequent rate-limiting transition state, the phosphoryl group would still be in a higher state of protonation than the reactant. Thus, the normal  $^{18}k_{\text{nonbridge}}$  is consistent with a mechanism in which the phosphate reactant becomes deprotonated, but not with the mechanism of Figure 2.

We considered the possibility that the normal  $^{18}k_{\text{nonbridge}}$  could be the result of a mechanism like that shown in Figure 2, but in which the inverse EIE for protonation is masked by a large normal (~3%) KIE in a phosphorane-like transition state, as in reactions of phosphotriesters.<sup>17</sup> Such a mechanism might serendipitously result in an observed net value for  $^{18}k_{\text{nonbridge}}$  resembling that for deprotonation. We measured the entropy of activation to ascertain the likelihood of a triester-type mechanism. Large negative entropies of activation characterize phosphotriester hydrolysis reactions. For example, for trimethyl phosphate hydrolysis,  $\Delta S^\ddagger = -23$  eu, and for triethyl phosphate,  $\Delta S^\ddagger = -34$  eu.<sup>30</sup> The hydrolyses of phosphate monoester monoanions, on the other hand, are characterized by very small

negative entropies of activation; for methyl phosphate monoanion hydrolysis  $\Delta S^\ddagger = -2.2$  eu; for phenyl phosphate  $\Delta S^\ddagger = -0.6$  eu.<sup>1</sup> We obtained a value of  $+28 \pm 1$  eu for the entropy of activation for the hydrolysis of the *m*NBP monoanion. The reason for the unexpectedly large positive value is uncertain, but it argues strongly against a triester-like mechanism.

The small inverse  $^{18}k_{\text{bridge}}$  of  $0.9981 \pm 0.0002$  for the hydrolysis of the monoanion of *m*NBP contrasts with the normal  $^{18}k_{\text{bridge}}$  of  $1.0087 \pm 0.0003$  for *p*NPP.<sup>3</sup> This KIE is the net value resulting from the normal contribution arising from P–O(R) bond fission, and the inverse value from protonation. The net replacement of the phosphoryl group of the reactant with hydrogen will result in a normal  $^{18}K_{\text{bridge}}$  EIE due to the loss of bending and torsional modes. (For similar reasons, the <sup>18</sup>O fractionation factors between water and alcohols are 2% to 3% normal (1.02 to 1.03), in the direction from alcohol to water).<sup>31</sup> To estimate the magnitude of this contribution to  $^{18}k_{\text{bridge}}$ , we calculated the gas phase <sup>18</sup>O fractionation factor between *p*-nitrophenol and *p*NPP, and that between *p*-nitrophenol and *p*-nitrophenyl acetate. The calculated value between *p*-nitrophenol and *p*-nitrophenyl acetate is 1.014. An experimental value of 1.012 for this fractionation factor can be obtained from the reported EIE between *p*-nitrophenolate anion and *p*-nitrophenyl acetate in water (0.9730)<sup>32</sup> and the EIE for protonation of *p*-nitrophenol, (0.9849).<sup>32</sup> The close agreement between the calculated and the experimental values supports the validity of the computational method, which gives a calculated EIE between *p*-nitrophenol and *p*NPP of 1.011. The experimental KIE for the hydrolysis of the *p*NPP monoanion (1.0087) approaches this value, consistent with a late transition state in which proton transfer to the leaving group and P–O(R) bond fission are both far advanced. In contrast, the small inverse  $^{18}k_{\text{bridge}}$  in the reaction of *m*-NBP suggests a transition state with less P–O(R) bond fission. In such a case, the inverse contribution from protonation will be less offset by loss of P–O(R) bond order and loss of bending and torsional modes associated with the phosphoryl group.

The conclusion that the transition state of the more reactive *p*NPP has significantly greater P–O(R) bond fission than the less reactive *m*NBP is counter to expectations based on the Hammond postulate. This apparent conundrum is resolved by recent computational results indicating that protonation of the P–O(R) ester oxygen atom weakens this bond to a degree that depends on the basicity of the ester group.<sup>10</sup> Comparison of the structures of the bridge-protonated anionic zwitterion forms of methyl and phenyl phosphates showed that in phenyl phosphate the P–O(R) ester bond is 0.24 Å longer than in the methyl ester.<sup>10</sup> Using Pauling's rule<sup>33</sup> and 1.6 Å as the distance for a P–O single bond, this constitutes a 60% weaker bond in the anionic zwitterion form of phenyl phosphate compared to that of methyl phosphate. These authors did not model bridge-protonated *p*-nitrophenyl phosphate, but presumably, the effect would be, if anything, even more pronounced. The experimental results here are consistent with the idea that protonation of the ester oxygen atom gives aryl phosphates a significantly greater “head start” on the way to P–O(R) bond fission relative to their

(27) Melander, L.; Saunders, W. H. In *Reaction Rates of Isotopic Molecules*; Wiley: New York, 1980; p 131.  
 (28) Melander, L.; Saunders, W. H. In *Reaction Rates of Isotopic Molecules*; Wiley: New York, 1980; p 152.  
 (29) Czyrca, P. G.; Hengge, A. C. *Biochim. Biophys. Acta* **2001**, *1547*, 245.  
 (30) Kluger, R.; Taylor, S. D. *J. Am. Chem. Soc.* **1990**, *112*, 6669.

(31) Rishavy, M. A.; Cleland, W. W. *Can. J. Chem.* **1999**, *77*, 967.  
 (32) Hengge, A. C.; Hess, R. A. *J. Am. Chem. Soc.* **1994**, *116*, 11256.  
 (33) Pauling, L. In *The Nature of the Chemical Bond*, 3rd ed.; Cornell University Press: Ithaca, NY, 1960; p 255.

alkyl counterparts, accounting for the transition state difference implied by the KIE data.

We previously<sup>3</sup> interpreted <sup>18</sup>O and <sup>15</sup>N KIE data for *p*NPP in terms of a concerted mechanism (Figure 1B), on the basis of a small <sup>15</sup>N KIE indicative of a small amount of negative charge on the leaving group in the transition state, suggesting that proton transfer and P–O bond fission might not be fully synchronous. However, the  $k_{\text{H}_2\text{O}}/k_{\text{D}_2\text{O}}$  KIE measured here does not support such a view, and the small <sup>15</sup>N KIE may reflect an EIE between *p*-nitrophenol (which the leaving group resembles in the very late transition state) and the *p*NPP reactant. On the basis of the collected evidence, the switch from preequilibrium proton transfer to concerted proton transfer/P–O bond fission probably occurs somewhere between the leaving groups *p*-nitrophenol ( $\text{p}K_{\text{a}} = 7.14$ ) and 2,4-dinitrophenol ( $\text{p}K_{\text{a}} = 4.07$ ).

In summary, the data presented here are most consistent with a pre-equilibrium proton transfer from the phosphoryl group to the ester oxygen atom, followed by rate-limiting P–O bond fission, for both *p*NPP and *m*NBP. The results also support computational predictions of differential effects of protonation on the P–O(R) ester bond, which are reflected in a substantial

difference in the extent of P–O(R) bond fission in the transition states for hydrolysis of the aryl ester *p*NPP compared to the alkyl *m*NBP. The data argue against a mechanism involving protonation of the reactant, such as that in Figure 2.

**Acknowledgment.** The authors thank the NIH for financial support (GM47297 to A.C.H.). The authors gratefully acknowledge the use of equipment in the Shimadzu Analytical Sciences Laboratory at Utah State University, created with equipment donated by Shimadzu Scientific Instruments, Inc. (Columbia, MD).

**Supporting Information Available:** Detailed procedures for <sup>18</sup>O isotope effect measurements, and levels of isotopic incorporation of *m*NBP isotopic isomers. Structures in z-matrix format and Gaussian 98 output with vibrational frequencies calculated for isotopomers of *p*-nitrophenol, *p*-nitrophenyl acetate, and *p*-nitrophenyl phosphate. This material is available free of charge via the Internet at <http://pubs.acs.org>.

JA036571J